

Regenerative Potential of Botox Combined and Uncombined with Platelet-Rich Plasma in Treating Induced Osteoarthritis of Temporomandibular Joint in Albino Rats

Original
Article

Dina M. Makawi¹, Nahed S. Korany², Nehad S. Taha¹ and Marwa M. S. Abbass²

¹Department of Oral Biology, Faculty of Oral and Dental Medicine, Misr International University.

²Department of Oral Biology, Faculty of Dentistry, Cairo University, Cairo, Egypt.

ABSTRACT

Objectives: One of the common therapeutic approaches for osteoarthritis is intra-articular injection due to the benefit of local drug delivery as well as instant pain relief. The aim of this study was to investigate the regenerative potential of intraarticular injections of Platelet-Rich Plasma (PRP), Botox and Botox + PRP (combined) in treating induced temporomandibular joint (TMJ) osteoarthritis in albino rats.

Design: Osteoarthritis was induced in rats by injection of 2mg monosodium iodoacetate in both sides of TMJ. After confirmation of osteoarthritis by enzyme-linked immunosorbent assay (ELISA), the rats were randomly divided to three groups. The right side acted as the experimental treatment group and was injected weekly with either Botox (5 IU/kg diluted in 50 µL saline), 50 µL PRP, or their combination, while the left side acted as control. Tissues were assessed at two and four weeks post-treatment histologically, radiographically and biochemically (using qRT-PCR and ELISA).

Results: The treated sides showed statistically significantly higher mean bone area percentages, in addition to lower statistically significantly mean IL-1 β and MMP13 levels than the untreated sides. The highest mean bone area % was recorded in the PRP group followed by the combined group of Botox+ PRP. The treated sides recorded a higher mean joint space than the untreated sides that is statistically significant in the Botox group ($p < 0.001$) and statistically non-significant in the PRP and Botox+ PRP group.

Conclusion: This study confirms the regenerative potential of PRP alone and in combination with Botox, which implies that the use of PRP alone or combined with Botox for treatment of TMJ osteoarthritis cases may enhance the healing potential of the condition.

Received: 03 December 2020, **Accepted:** 18 February 2021

Key Words: Botox, osteoarthritis, platelet-Rich Plasma, temporomandibular joint.

Corresponding Author: Dina M. Makawi, PhD, Department of Oral Biology, Faculty of Oral and Dental Medicine, Misr International University, Egypt, **Tel.:** +20 10061 53310, **E-mail:** dina.mekawy@miuegypt.edu.eg

ISSN: 1110-0559, Vol. 45, No.1

INTRODUCTION

The temporomandibular joint (TMJ) is a synovial joint that performs the most complicated movement in the human body^[1]. Temporomandibular disorders (TMDs) are defined as a group of pathological changes that can affect different structures of the stomatognathic system, such as TMJ and masticatory muscles^[2].

TMDs have conventionally been treated with intraoral appliances, occlusal adjustments, dental restoration and/or surgery^[3]. These techniques are invasive, irreversible and expensive. Moreover, conservative restorative treatments may not withstand the parafunctional forces continually applied by some patients^[3].

Osteoarthritis is among the common diseases affecting the TMJ. It affects women more than men and is more prevalent in older age groups^[4]. TMJ osteoarthritis shows an increase in cartilage degradation, subchondral bone remodeling and chronic inflammation in the synovial tissue^[1].

Up till now, there is no ultimate therapy for OA, meaning that current treatment focuses on ways to treat patient symptoms and slow down the destruction process. The current treatment goals for OA focus on enhancing the function of the joint and reducing pain levels and stiffness, avoiding further deformities in the joint and in general improving the quality of life for the patients^[5].

The pharmacological therapies commonly used in treatment of OA cases include anti-inflammatory gels; oral non-steroid anti-inflammatory drugs (NSAIDs); oral supplements, such as glucosamine and chondroitin sulfate besides injection therapies. The injection therapies currently used include corticosteroids, hyaluronic acid (HA), platelet-rich plasma (PRP), and injections using patients own mesenchymal stem cells (MSCs). For patients that do not respond to such pharmacological therapeutic measures, surgical approach is then considered such as arthroscopic surgery and osteotomy^[6].

Intra-articular injection of corticosteroids is one of the common treatment modalities for osteoarthritis^[7]. However several drawbacks have been reported for the long-term use of corticosteroids, such as joint destruction and toxic effects of the surrounding tissues and cartilage^[8]. Therefore, there is a need for alternative therapies for osteoarthritis.

To achieve the ultimate non-invasive treatment for OA, a promising injective treatment, PRP appeared in the clinical field. PRP is a blood derivative that is rich in platelets. These platelets when activated release a group of active proteins that act to promote cellular recruitment, growth and morphogenesis as well as modulate inflammation. PRP represents a promising biological approach to enhance tissue healing of structures that have a healing power, as cartilage. PRP also showed highly favorable outcomes as intra-articular injection for treatment of cases as cartilage breakdown and OA^[9,10].

PRP is also gaining a lot of interest in different treatment modalities as it is considered well tolerated, very rarely leads to complications, easy to prepare and it is less invasive than other treatment options that might be indicated for such cases, as corticosteroid therapy or even surgical approach^[11].

Botox (BTX) is another minimally invasive procedure that gained great interest recently in the dental field due to its benefits in treating various oral conditions such as TMDs, bruxism, mandibular spasm, and masseteric hypertrophy^[12]. BTX is a type of a neurotoxin produced by Clostridium botulinum, which acts by blocking the neuromuscular junction and preventing acetylcholine release into the synaptic cleft, leading to chemical denervation that eventually causes flaccid paralysis^[13].

In view of these facts, this study was carried out to investigate the anti-inflammatory effect and regenerative potential of two non-invasive regimes of treatments in treating induced TMJ osteoarthritis: PRP, Botox and a combination of both in Albino rats. PRP^[14] and BTX^[15] has been shown to be useful for TMJ osteoarthritis in patients. To our knowledge, there is no documented study that compares between the biological effects of PRP and

Botox separately and combined in treating the induced osteoarthritis of TMJ in *vivo*.

MATERIALS AND METHODS

This study was approved by Institutional Animal Care and Use Committee (IACUC) in Cairo University (CU-III-F7417). Forty-two male adult Wister albino rats with an age from 3-4 months (180 to 200 grams) were obtained from the Faculty of Medicine, Cairo University. All animals were housed in a sterile, controlled environment at a temperature of 28 to 35°C and maintained throughout the experiments on a 12:12 h light-dark cycle. The rats were fed pellets and fresh tap water. The 42 rats were randomly distributed into three experimental groups (Figure 1) according to the type of given treatment; each containing 14 rats (Table 1): Group I (Botox group), Group II (PRP group) and Group III (Botox + PRP group). All rats were also injected with 0.05 ml of saline in the left side TMJ as an intra-articular injection weekly.

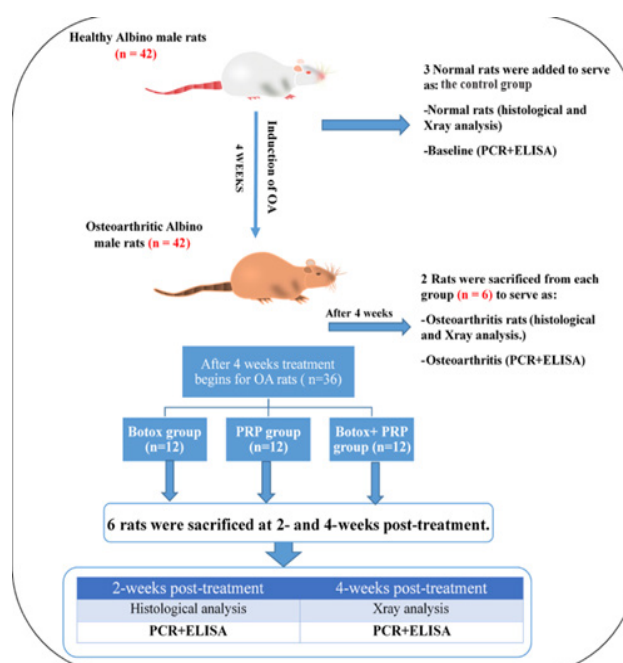


Fig. 1: Diagram illustrating the animal allocating and grouping.

Table 1: The complexity of the study design

		Group I		Group II		Group III		Control group	
No. of Rats		14		14		14		3	
TMJ side		Right	Left	Right	Left	Right	Left	Right	Left
Induction of OA	Route	2 mg of monosodium iodoacetate						-	
	Dose	Single intra-articular injection						-	
Treatment begins (After 4W from induction of OA)		Botox 5 IU/kg (0.05ml)	Saline (50 µL) (0.05ml)	PRP 50 µL (0.05ml)	Saline (50µL) (0.05ml)	Botox +PRP	Saline (50µL) (0.05 ml)	-	
Date of sacrifice		2- and 4 weeks post-treatment						Prior to induction of OA	

Additional 3 rats were considered as normal control group using the right and left TMJs (6 specimens) to detect baseline levels before the induction of osteoarthritis.

Right and left TMJs of all rats were dissected, with half of the tissues kept in 10% neutral formalin for histological and Xray analysis, while the other half were frozen to be used for quantitative real time polymerase chain reaction (qRT-PCR) and enzyme-linked immunosorbent assay (ELISA) to detect levels for matrix metalloproteinase-13 (MMP-13) and Interleukin 1 beta (IL-1 β) respectively.

Methods and interventions

1.1 Osteoarthritis induction

On the first day of the experiment, all rats were generally anesthetized with intraperitoneal injection of chloral hydrate (370-400 mg/g body weight). Rats were injected intra-articularly with 2 mg of monosodium iodoacetate (MIA) as a single dose dissolved in 50 μ l saline using a 27-gauge 0.5-inch needle in the right and left side TMJ of each group to induce osteoarthritis^[16,17]. The right side was designated as the treated group while the left side acted as the untreated control.

1.2 Confirmation of osteoarthritis induction

After 4 weeks, two rats from each experimental group were sacrificed and their left and right TMJs were harvested. Confirmation of osteoarthritis induction was done through biochemical analysis of IL-1 β using ELISA, and levels of IL-1 β protein expression were compared to its normal levels collected before induction of osteoarthritis^[18,19].

The remaining 12 rats from each group will be divided into 3 groups according to the given treatment: Group I (Botox group), Group II (PRP group) and Group III (Botox + PRP group).

1.3 Botox® (Onabotulinum toxin A; Allergan, USA) injection

Treatment with Botox® was started after confirmation of osteoarthritis as a weekly single intra-articular injection of 5 units/kg (0.05ml) diluted in 50 μ L saline into the upper compartment of right side TMJs^[16,17].

1.4 PRP preparation and injection

Blood samples were obtained from the retro-orbital plexus or peri-orbital method^[20]. For PRP preparation, blood samples were collected into sterile tubes and single centrifugation protocol was applied as it was proven to yield higher platelet count and concentration than double spin centrifugation protocol^[21], and then immediately injected in the right side of TMJ of the rats^[21,22]. The PRP volume administered was the same for all animals (50 μ L).

1.5 Post-mortem specimens processing

Six rats from each group were sacrificed at 2- and 4-weeks post-treatment. At 2 weeks for histological and biochemical analysis and at 4 weeks for Xray and

biochemical analysis. Animals were euthanized by intraperitoneal injection of 200 mg/kg sodium phenobarbital^[23].

Cone beam computed tomography (CBCT) scan analysis

At 4-weeks post-treatment, rats were subjected to X-ray imaging prior to tissue dissection. CBCT images were obtained for the rats using CRANEX 3D (SOREDEX, Tuusula, Finland), the specimens were scanned with 80 KV and 10 mA. Three-dimensional analysis was performed using the system's software (OnDemand). The joint space between head of condyle and temporal bone was measured at 3 different points for each side of TMJ in each group then analyzed.

Histopathological examination

Histopathological examination was performed for tissues at 2-weeks post-treatment. Specimens were immediately fixed in 10% neutral formalin for 48 h and then rinsed in distilled water. Specimens were then decalcified^[24] and subsequently stained with hematoxylin and eosin according to the conventional method^[25]. Histopathologic examination was performed using light microscopy.

Histomorphometric analysis

Hematoxylin and eosin-stained sections were examined by Leica Quin 500 analyzer automated computer software. The image analyzer was calibrated automatically to convert the measurement units (pixels) produced by the image analysis program into actual micrometer units. Staining was measured as percentage area of bone tissue area over total tissue area in 10 separate fields in each group using x20 magnification. Areas of bone showing the most uniform staining was chosen for evaluation. The areas were then masked by a blue binary color to be quantified by the computer system.

Enzyme-linked immunosorbent assay (ELISA)

ELISA technique was utilized for assessment of gene expression levels of IL-1 β at 2- and 4-weeks post-treatment. Samples of TMJ were dissected, snap frozen in liquid nitrogen and then stored at -40°C. Sample processing was done using the Rat IL-1 β ELISA kit (RayBio®, Catalog #: ELR-IL1 β). IL-1 β levels (pg/ml tissue) were assessed in tissue homogenate according to the manufacturer's instructions.

Quantitative real time –polymerase chain reaction (qRT-PCR)

Dissected frozen specimens were used for detection of MMP-13 protein expression to reflect the amount of cartilage degradation at 2- and 4-weeks post-treatment.

6.1 RNA Extraction

RNA extraction was performed using the Gene JET Kit (#K0732; ThermoFisher Scientific, Germany).

6.2. qRT-PCR

The cDNA amplification was performed using the SensiFAST™ SYBR® Hi-ROX One-Step Kit (catalog no.PI-50217 V, Bioline, UK). Prepared reaction samples were applied in real time PCR (StepOne Applied Biosystem, USA). The amplification procedure involved three-step cycling; 10 mins(45°C) for reverse transcription, 2 mins (95°C) for polymerase activation followed by 40 cycles for 5s (95°C) for denaturation;10s (60°C) for annealing and finally 5s (72°C) for extension. After the RT-PCR, the data were expressed in cycle threshold (Ct). The PCR data sheet includes Ct values of assessed gene (MMP-13) and the house-keeping gene (GAPDH). Relative quantitation (RQ) of each target gene was quantified according to the calculation of delta-delta Ct ($\Delta\Delta Ct$) method. Primers sequence specific for each gene from 5'- 3':

MMP-13: F: TACAGAATTGTGAACTACAC,
R: AAAGAACATGGTGACTTCTA

GAPDH: F: GACGGCCGCATCTTCTTGA,
R: CACACCGACCTTCACCATTTT

Statistical analysis

Data was assessed for normality by checking the distribution of data and using Kolmogorov-Smirnov and Shapiro-Wilk tests. All data showed normal (parametric) distribution. Data is presented as mean \pm standard deviation (SD) values. Repeated measures analysis of variance (ANOVA) was used for multiple comparisons while Bonferroni's post-hoc test is used for pair-wise comparisons when ANOVA test is significant. The significance level was set at $p \leq 0.05$. Statistical analysis was performed using IBMSPSS Statistics Version 20 for Windows (IBM Corporation, USA).

RESULTS

Histopathology analysis

1.1. Normal rat TMJ

Histopathological examination of the rat's normal TMJ (Figures 2A,C) showed TMJ components: condyle, intra-articular disk and temporal bone. The temporal bone was covered with a uniform fibrous layer that separated it from the underlying bone, composed of interconnected plates of spongy bone. The disc showed normal appearance; thin at its central part and thickened at both ends (biconcave; Figure 2A). The condyle showed normal anatomy and outline. Its articular surface was covered by fibrous layer, proliferative layer, fibrocartilaginous zone and calcified cartilage zone (Figure 2C). The underlying subchondral bone showed normal interconnecting bone trabeculae (Figure 2C) with few bone marrow spaces.

1.2. Osteoarthritis rat TMJ

The temporal bone appeared ankylosed with the underlying disc and condyle. Widened marrow spaces with chronic inflammatory cells was observed in the temporal bone (Figure 2B). The proliferative zone appeared with

acellular areas (Figure 2D). The calcified cartilage layer showed chondrocytes with mitotic figures, empty lacunae and hypertrophic chondrocytes (Figure 2D). The subchondral bone showed widened marrow spaces with chronic inflammatory cells.

1.3. Group I (Botox group)

The right (treated) side revealed the intra-articular disc with normal thickness, but fibrillation appeared at both ends (Figure 3A). The temporal bone showed typical size marrow spaces with chronic inflammatory cells (Figure 3A). The Proliferative zone appeared with chondrocytes showing mitotic figures and the calcified cartilage zone showing empty lacunae and hypertrophic chondrocytes (Figure 3C).

Examination of the left side untreated; revealed notable deformation in the condyle architecture with matrix discontinuity and erosion (Figure 3B). The disc appeared quite thin at central part with fibrillation at its ends. The temporal bone revealed narrow bone marrow spaces (Figure 3B) with local thickening of its fibrous covering. The fibrocartilaginous and calcified cartilage zone showed smaller than normal size chondrocytes with random orientation and focal loss (Figure 3D). Subchondral bone showed many reversal lines (Figure 3D).

1.4. Group II (PRP group)

The right side (treated) revealed temporal bone with normal fibrous covering and few marrow spaces (Figure 4A). The intra-articular disc appeared thin at its central part and thickened at both ends (Figure 4A). The condyle's bone trabeculae appeared normal with appearance of vertical and horizontal fissures in the subchondral bone area (Figure 4A). All the condyle layers revealed focal cellular loss in some areas. Calcified cartilage layer showed clusters of chondrocytes, however lacked empty lacunae or mitotic figures (Figure 4C).

The left untreated side revealed normal appearance of the temporal bone. The disc appeared quite thin at its central part that is nearly cut (Figure 4B). The fibrous zone appeared separated from the underlying layer (Figure 4B). The fibrous zone appeared with few cracks as well as acellular areas in the fibrocartilaginous layer (Figure 4D). The calcified cartilage layer appeared with some chondrocytes showing mitotic figures, while others appeared hypertrophic (Figure 4D).

1.5 Group III (Botox +PRP group)

The right (treated) side exhibited normal appearance of the temporal bone. The disc appeared with a thickened central part, normal thickened anterior and thinned posterior ends with marked fibrillation (Figure 5A). The condyle showed normal bone trabeculae and marrow spaces, surface discontinuity at the posterior part of the condyle and gradual loss of chondrocytes (Figure 5A). The fibrous zone appeared nearly acellular in some areas while the proliferative zone showed normal cellular appearance

(Figure 5C). The fibrocartilaginous layer showed focal loss of chondrocytes and the calcified cartilage zone appeared with no mitotic figures or empty lacunae (Figure 5C).

The left untreated control side revealed discontinuity in the temporal bone's fibrous covering with horizontal and vertical fissures. The disc appeared quite thin at its central part, normal thickness at both ends (Figure 5B). The fibrous layer appeared nearly acellular, the proliferative layer with normal cellular appearance and few acellular areas while, the fibrocartilaginous layer appeared with hypertrophic chondrocytes and empty lacunae (Figure 5D).

Histomorphometric analyses

In all groups, the treated side showed statistically significant higher mean bone area % than untreated side ($p < 0.001$; Table 2). 2 weeks post-treatment, there was no statistically significant difference between normal and PRP-treated samples ($p = 0.915$), with both showing the highest mean bone area % values. Botox-treated samples showed a statistically significant lower mean bone area % than the other two treated groups ($p < 0.001$).

Xray results (Radiographic analysis using CBCT scan)

3.1. Normal rats

The coronal 3D and 2D CT images (Figure 6A,B) revealed normal appearance of the condyle head in relation to the condyle fossa in the right and left side TMJ with obvious appearance of normal width of the joint space (Table 3).

3.2. Osteoarthritis rats

The coronal CT 3D and 2D images (Figure 6C,D) revealed ankylosis of both sides of the condylar head in relation to the glenoid fossa. Statistical analysis comparing the normal and osteoarthritis mean joint space revealed a statistically significant difference ($P < 0.001$) (Table 3).

3.3. Experimental Groups,

The radiographic analysis for both sides revealed: narrowing of the joint space between the condyle head in relation to the glenoid fossa in the right and left TMJ but more narrowing was observed in the left side TMJ in Botox group (Figure 6E,F) and PRP group (Figure 6G,H). On the other hand, Botox+PRP group (Figure 6I, J) revealed normal joint space in three right side TMJ, while the left side TMJ showed narrowing toward the midline. The treated sides recorded a higher mean joint space than the untreated sides that is statistically significant in the Botox group ($p < 0.001$) and statistically non-significant in the PRP and Botox+PRP group ($p = 0.065$, $p = 0.064$, respectively) (Table 3).

ELISA results for IL-1 β

In all experimental groups, the treated side either after 2 or 4 weeks post-treatment in Botox, PRP, Botox+PRP groups revealed statistically significantly lower mean IL-1 β levels than the control side ($p < 0.001$) (Tables 2,3). Moreover, comparison between all groups at both time intervals showed that the PRP (untreated side) showed the statistically significant highest mean IL-1 β levels (435.0) (Tables 2,3).

qRT-PCR results for MMP13

Treated sides showed statistically significantly lower mean MMP-13 levels than the untreated control sides in all experimental groups either after 2- or 4-weeks post-treatment. Comparison between all groups showed that at 2 weeks post-treatment; there was no statistically significant difference between Botox (untreated side) and Botox + PRP (untreated side) ($p = 0.885$); both showed the statistically significantly highest mean MMP13 levels (4.16 and 4.21 respectively) (Table 2). On the other hand, 4 weeks post-treatment PRP (untreated side) showed the statistically significant highest mean (7.08) MMP13 levels in comparison to all other groups (Table 3).

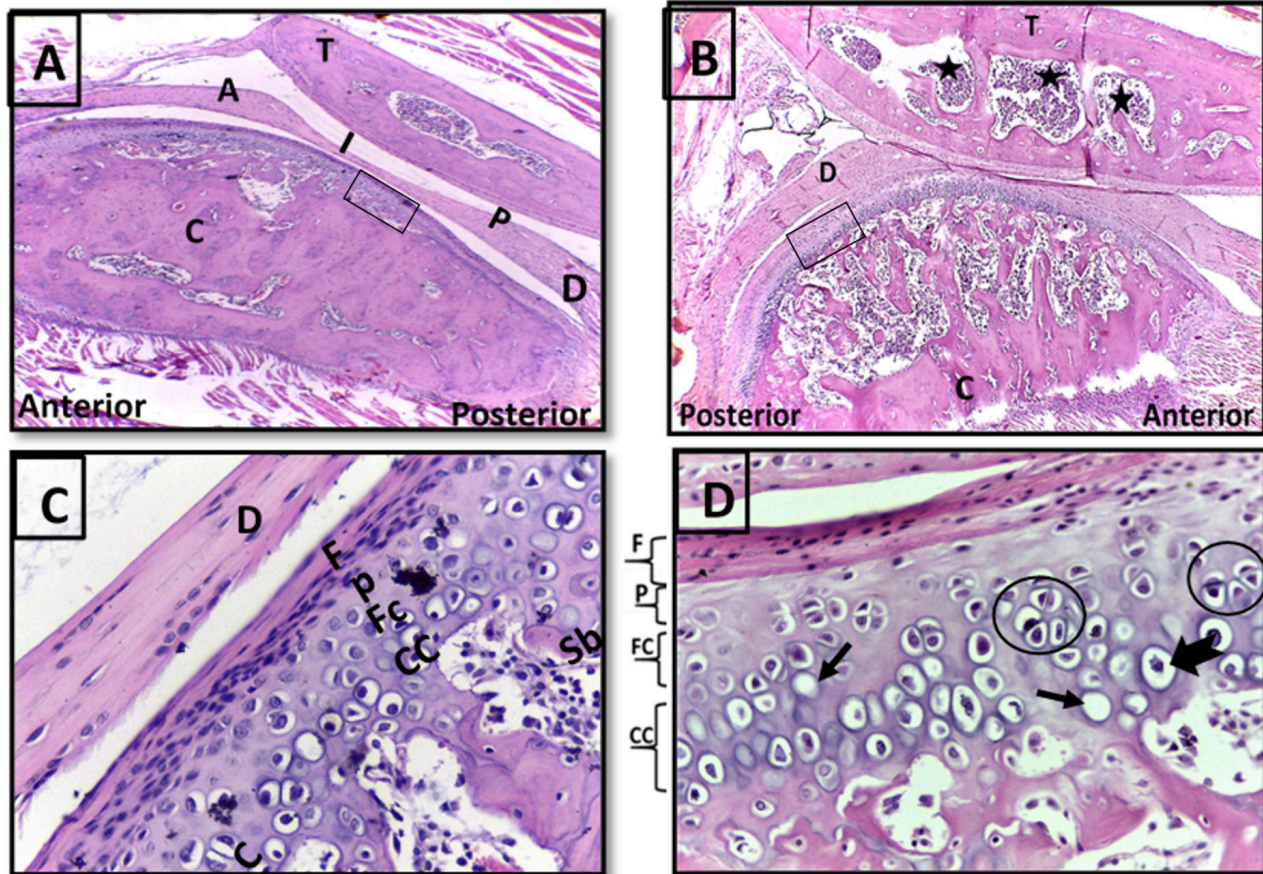


Fig. 2: Photomicrographs of sagittal section in TMJ from normal (A, C) and osteoarthritic rats' TMJ (B, D) showing:
 A) Normal rats' TMJ revealed: nearly normal configuration of the TMJ with normal appearance of temporal bone (T), intra-articular disc (D) and condyle (C). The disc was divided into three regions: Intermediate thinnest region (I), anterior (A) and posterior thick regions (P). (H&E, Orig.Mag.x4)
 B) Osteoarthritic rats TMJ revealed: temporal bone (T) ankylosed with underlying intra-articular disc (D) and condyle (C). Temporal bone with widened marrow spaces filled with chronic inflammatory cells (asterisks). The disc appeared ankylosed at its central part to the overlying temporal bone and the underlying condylar head (H&E, Orig.Mag.x 4).
 C) Photomicrograph of higher magnification of the rectangular area in Fig. 2A showing: intra-articular disc (D) and condyle (C) with its fibrous covering (F), proliferative layer (P), fibrocartilaginous zone (FC), calcified cartilage (CC) and the underlying subchondral bone (Sb) (H&E, Orig.Mag.x40).
 D) Photomicrograph of higher magnification of the rectangular area in Fig. 2B showing: the 4 zones of the condylar head: fibrous zone (F), proliferative zone(P), fibrocartilaginous zone (FC), calcified cartilage (CC) or hypertrophic zone. The proliferative zone appeared with acellular areas (asterisk). The cartilage layer showed chondrocytes with mitotic figures (circles), empty lacunae (arrows) and hypertrophic chondrocytes (notched arrows) (H&E, Orig.Mag.x40).

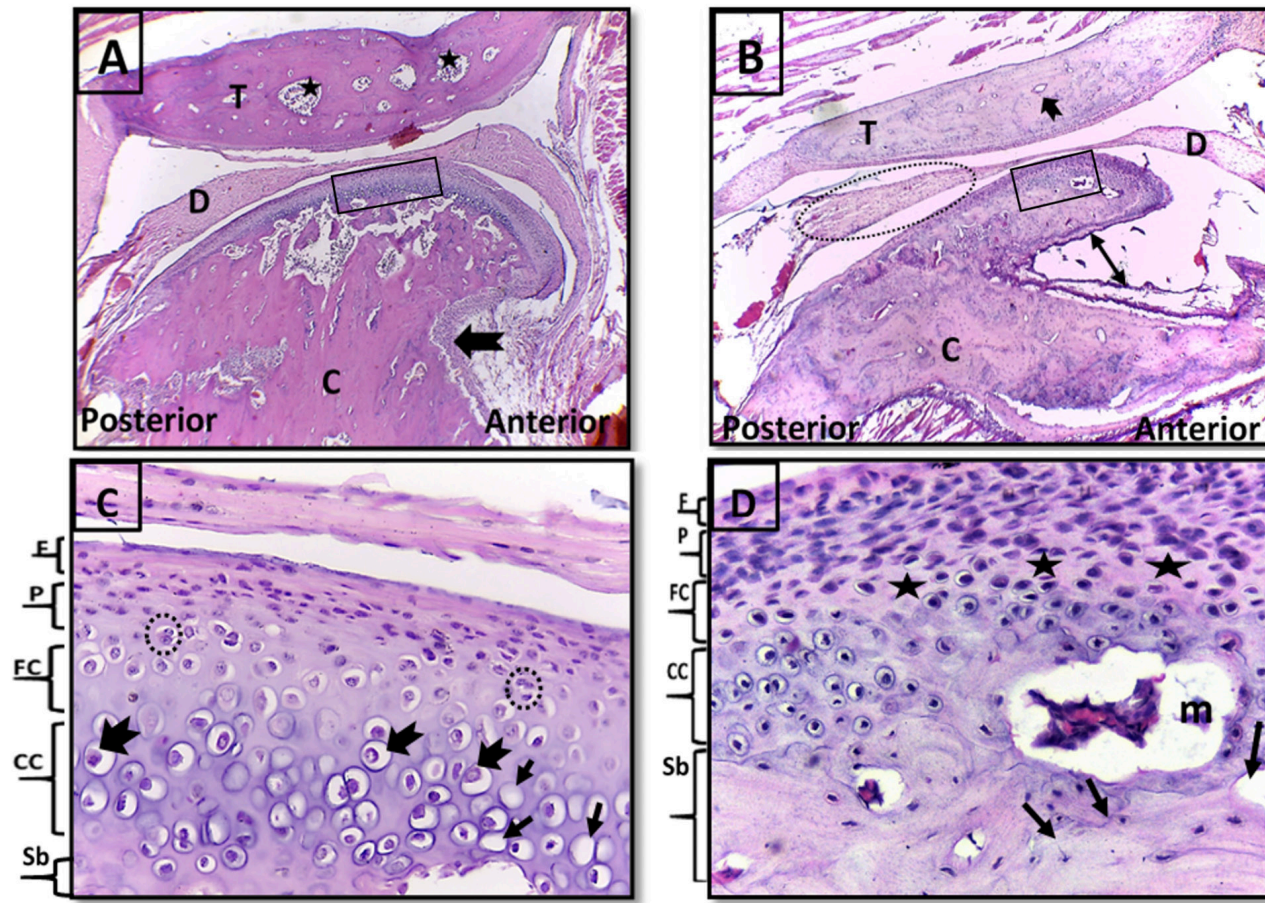


Fig. 3: Photomicrographs of sagittal section in TMJ from group I (Botox) Figs (A, C) (treated sides), Figs (B, D) (untreated sides), showing:

A. The condyle (C) showed numerous bone marrow spaces filled with chronic inflammatory cells and surface erosion (notched arrow). In temporal bone (T) relatively normal size marrow spaces filled with chronic inflammatory cells (asterisks). The disc (D) appeared thin at its central part and thickened at its posterior and anterior ends with obvious fibrillation. (H&E, Orig.Mag.x4).

B. The condyle (C) showed huge area of deformity, fibrillation, matrix discontinuity and erosion (double headed arrow) in the middle part. The temporal bone (T) appeared normal but with very narrow marrow spaces (notched arrow). The disc (D) appeared thin at its central part and thickened at its posterior and anterior ends with abnormal fibrillation at its posterior end (dotted circle) (H&E, Orig.Mag.x4).

C. Photomicrograph of higher magnification of the rectangular area in Fig. 3A showing the condyle's articular surface of the treated side with the 4 zones of the condylar head: fibrous zone (F), proliferative zone (P), fibrocartilaginous zone (FC) and calcified cartilage (CC) or hypertrophic zone. The proliferative layer showed chondrocytes with mitotic figures (dotted circles), while the calcified cartilage layer showed empty lacunae (arrows) and hypertrophic chondrocytes (notched arrows). (H&E, Orig.Mag.x40).

D. Photomicrograph of higher magnification of the rectangular area in Fig. 3B showing the condyle's articular surface of the untreated side with the 4 zones of the condylar head: fibrous zone (F), proliferative zone (P), fibrocartilaginous zone (FC) and calcified cartilage (CC). The fibrocartilaginous and calcified cartilage zone showed chondrocytes with random orientation and focal loss of chondrocytes (asterisks) they also appeared smaller than normal in size. Subchondral bone (Sb) showed marrow spaces (m) filled with few chronic inflammatory cells and many reversal lines (arrows) (H&E, Orig.Mag.x40).

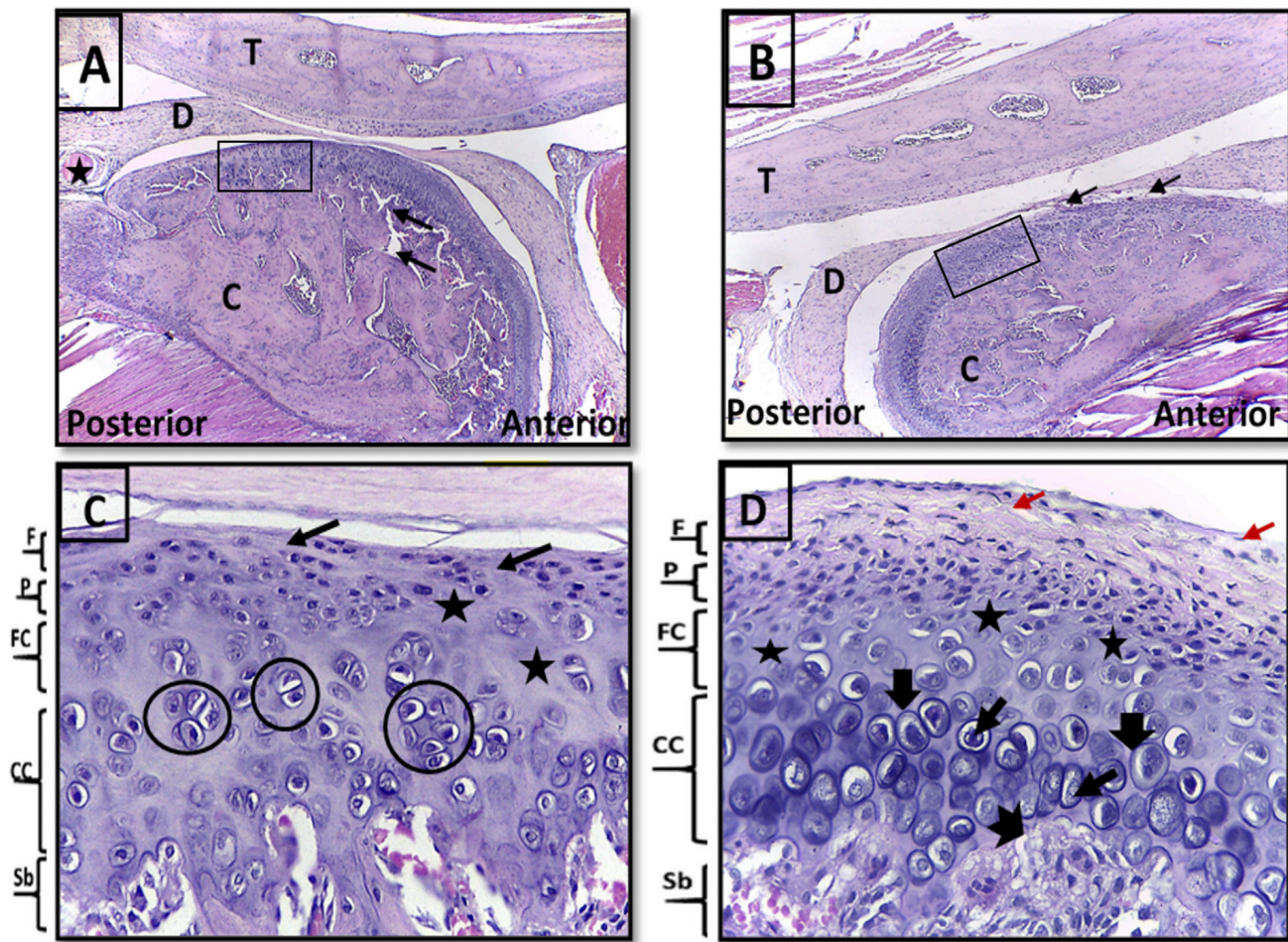


Fig. 4: Photomicrographs of sagittal section in TMJ from group II (PRP) Figs (A, C) (treated sides), Figs (B, D) (untreated sides), showing:

A. Temporal bone (T) with normal fibrous covering and few bone marrow spaces. Intra-articular disc (D) with normal appearance and thickness, congested blood vessels (asterisk) at the posterior end. The condyle (C) with more or less normal bone trabeculae, enclosed marrow cavities with chronic inflammatory cells. Vertical and horizontal fissures in the subchondral bone area (arrows) (H&E, Orig.Mag.x4).

B. Temporal bone (T) with normal fibrous covering and widened bone marrow spaces. Intra-articular disc (D) with quite thin central part and normal thickened anterior and posterior ends. The condylar (C) bone trabeculae enclosing marrow cavities with chronic inflammatory cells. Obvious loss of the fibrous covering near the central and posterior ends was seen (arrows) (H&E, Orig.Mag.x4).

C. Photomicrograph of higher magnification of the rectangular area in Fig. 4A showing the condyle's articular surface of the treated side. Focal loss of cells in fibrous layer (F) (thin arrows), proliferative layer (P) and fibrocartilaginous layer (FC) (asterisks). Calcified cartilage (CC) layer showed clusters of chondrocytes (circles). No empty lacunae or mitotic figures were seen. Subchondral bone (Sb) appeared with many marrow spaces (H&E, Orig.Mag.x40).

D. Photomicrograph of higher magnification of the rectangular area in Fig. 4B showing the condyle's articular surface of the untreated side. The fibrous zone (F) with few cracks (red arrows), proliferative layer (P) with normal cellular appearance. The fibrocartilaginous layer (FC) appeared with few acellular areas (asterisks). The calcified cartilage layer (CC) appeared to have chondrocytes with mitotic figures (thin arrows) and some appeared hypertrophic (thick arrow). Subchondral bone (Sb) appeared with many marrow spaces filled with chronic inflammatory cells, reversal lines were also obvious (notched arrow) (H&E, Orig.Mag.x40)

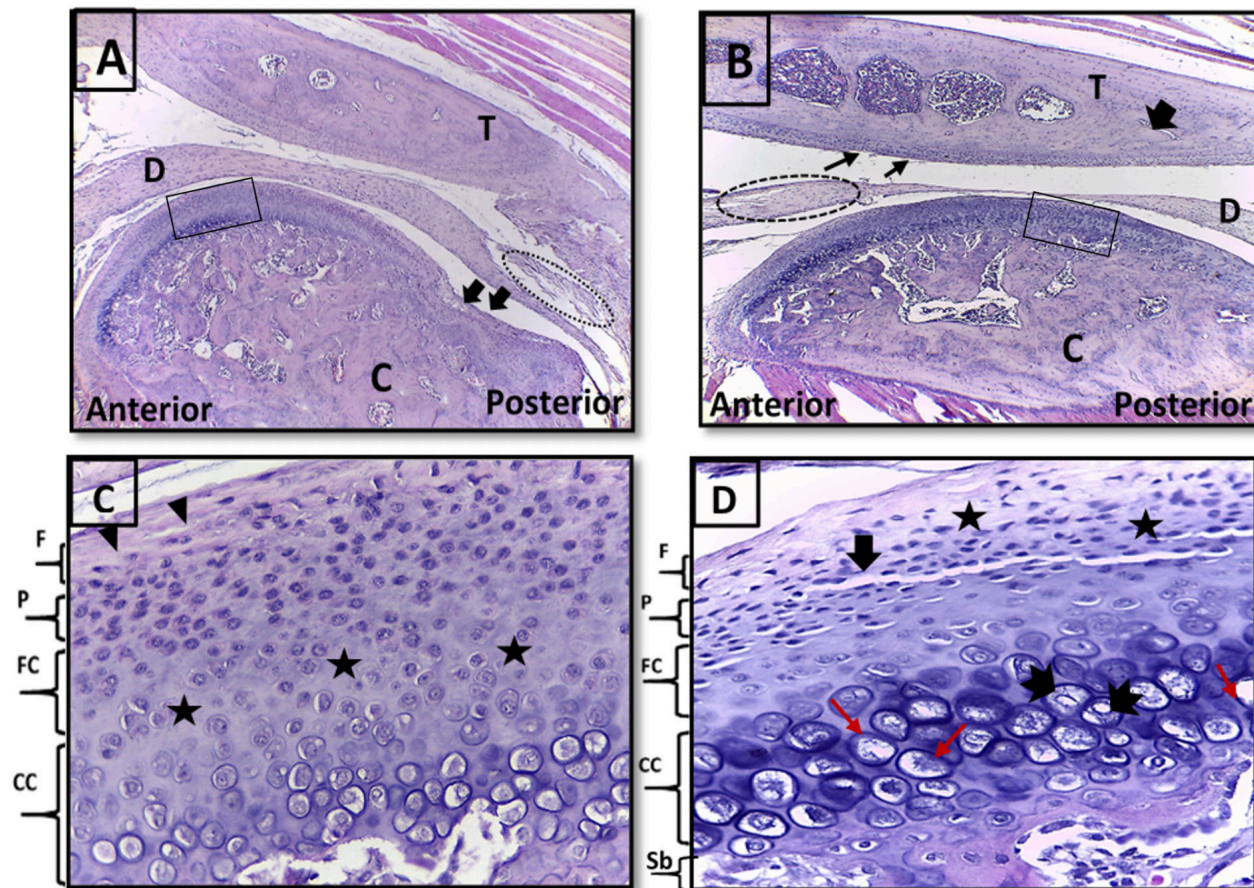


Fig. 5: Photomicrographs of sagittal section in TMJ from group III (Botox+PRP) Figs (A, C) (treated sides), Figs (B, D) (untreated sides), showing:

A. Temporal bone (T) with normal looking fibrous covering and normal bone marrow spaces filled with chronic inflammatory cells. Intra-articular disc (D) appeared normal but with quiet thickened central part and thinned posterior ends with obvious fibrillation (dotted circle). The condyle (C) was with normal bone trabeculae and bone marrow spaces, surface discontinuity at the posterior part of the condyle (thick arrows) (H&E, Orig.Mag.x4)

B. Temporal bone (T) with discontinuity in its fibrous covering (thin arrows), horizontal and vertical fissures (thick arrow) and wide bone marrow spaces with chronic inflammatory cells. Intra-articular disc (D) thin at its central part, normal thickness at the anterior and posterior ends with obvious fibrillation in its anterior end (dotted circle). The condyle (C) with normal bone trabeculae and bone marrow spaces (H&E, Orig.Mag.x4).

C. Photomicrograph of higher magnification of the rectangular area in Fig. 5A showing the condyle's articular surface of the treated side. Fibrous zone (F) with normal thickness but few cells and nearly acellular in some areas (arrowheads). The proliferative zone (P) with normal cellular appearance. The fibrocartilaginous layer (FC) with focal loss of chondrocytes (asterisks). The calcified cartilage (CC) zone with no mitotic figures or empty lacunae. (H&E, Orig.Mag.x40).

D. Photomicrograph of higher magnification of the rectangular area in Fig. 5B showing the condyle's articular surface of the untreated side. The fibrous layer (F) appeared nearly acellular, the proliferative layer (P) with normal cellular appearance but with large crack (thick arrow) and few acellular areas (asterisks). The fibrocartilaginous layer (FC) appeared with degenerated cells (thin arrows). The calcified cartilage (CC) zone with hypertrophic chondrocytes (notched arrows) and degenerated cells in relatively empty lacunae appearance (red arrows). Subchondral bone (Sb) appeared with many marrow spaces (H&E, Orig. Mag.x40).

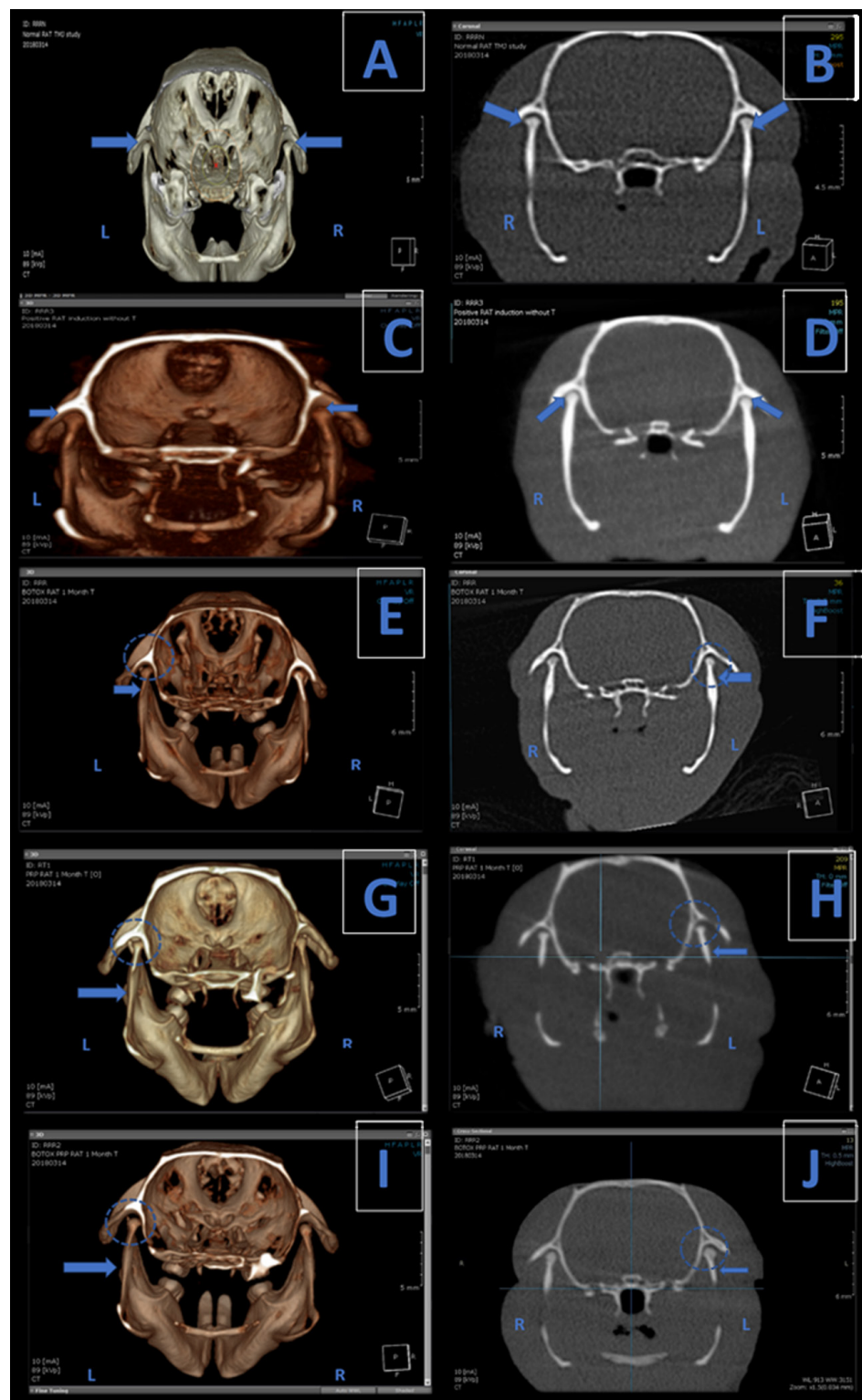


Fig. 6: A coronal CT image for TMJ of the rats, CBCT,3D figs (A, C, E, G, I) and CBCT,2D figs (B, D, F, H, J) showing: (A, B) CBCT (3D,2D) image for TMJ of the normal rats showing the condyle and glenoid fossa with their normal shape and angulation. The joint space appeared in both sides with no sign of ankylosis (arrows). (C, D) CBCT (3D,2D) images for TMJ of the osteoarthritis group, demonstrating bilateral joint space narrowing and ankylosis of the head of the condyle to glenoid fossa on both sides (arrows). (E, F) CBCT (3D,2D) images for Botox group, showing narrowing of joint space of the left TMJ with obvious angulation of the ramus toward midline (arrow). Slight narrowing of joint space of the right TMJ but with obvious angulation toward midline (dotted circle). (G, H) CBCT (3D,2D) images for PRP group, showing bony ankylosis at the left TMJ (dotted circle) with obvious angulation of the ramus and condyle toward midline (arrow). Slight narrowing of joint space of the right side TMJ and angulation toward midline but fewer than left TMJ. (I, J) CBCT (3D,2D) images for BOTOX+ PRP group, showing joint space narrowing at the left TMJ (dotted circle) toward the midline with obvious angulation at the ramus toward the midline (arrow). Slight narrowing of the joint space of the right side TMJ.

Table 2: Showing the mean, SD values of ANOVA test for comparison between bone area %, IL-1 β and MMP13 levels of the different groups at 2 weeks post-treatment.

Group	Bone area %		IL-1 β levels		MMP13 levels	
	Mean	SD	Mean	SD	Mean	SD
Normal	82.4 ^a	2.9	72.2 ^b	2.6	1.26 ^E	0.10
Osteoarthritis	41.5 ^c	2.9	321.3 ^d	4.4	3.55 ^B	0.25
Botox (Treated side)	63.7 ^e	4.8	205.3 ^f	10.6	2.24 ^C	0.13
Botox (Untreated side)	50.6 ^d	2	405.3 ^b	17.2	4.16 ^A	0.75
PRP (Treated side)	82.1 ^a	4.3	180.9 ^g	5.7	2.28 ^e	0.04
PRP (Untreated side)	64.2 ^c	5.2	435.0 ^a	9.8	3.58 ^b	0.62
Botox + PRP (Treated side)	69.5 ^b	2.2	193.5 ^e	7.5	2.20 ^e	0.11
Botox + PRP (Untreated side)	54.6 ^d	3.4	374.6 ^c	11.8	4.21 ^a	0.74
<i>P-value</i>	<0.001*		<0.001*		<0.001*	

*: Significant at $P \leq 0.05$, Different superscripts indicate significant differences

Table 3: Showing the mean, SD values of ANOVA test for comparison between Joint space, IL-1 β and MMP-13 levels of the different groups at 4 weeks post-treatment.

Group	Joint Space(mm)		IL-1 β levels		MMMP-13 levels	
	Mean	SD	Mean	SD	Mean	SD
Normal	0.43 ^A	0.09	72.2 ^G	2.6	1.26 ^G	0.10
Osteoarthritis	0.14 ^C	0.01	321.3 ^D	4.4	3.55 ^E	0.25
Botox (Treated side)	0.28 ^B	0.03	113.6 ^E	14.7	1.61 ^F	0.06
Botox (Untreated side)	0.15 ^C	0.02	464.6 ^C	12.0	6.17 ^B	0.05
PRP (Treated side)	0.37 ^{AB}	0.07	84.3 ^F	9.7	1.53 ^F	0.36
PRP (Untreated side)	0.26 ^B	0.02	509.7 ^A	14.9	7.08 ^A	0.21
Botox + PRP (Treated side)	0.31 ^B	0.03	81.4 ^F	5.2	1.60 ^F	0.38
Botox + PRP (Untreated side)	0.23 ^B	0.07	482.5 ^B	3.9	4.83 ^C	0.09
<i>P-value</i>	<0.001*		<0.001*		<0.001*	

*: Significant at $P \leq 0.05$, Different superscripts indicate significant differences

DISCUSSION

Osteoarthritis is a degenerative joint disease affecting millions of people worldwide. This continues to increase due to the increase in global life expectancy^[26].

The aim of the present study was to investigate and compare the anti-inflammatory effects and regenerative potential of PRP, Botox and the combination of both (PRP and Botox) in treating induced TMJ osteoarthritis in Albino rats. This was assessed using histological examination (2 weeks post-treatment), X-rays (4 weeks post-treatment), qRT-PCR for MMP-13 and ELISA for IL-1 β protein levels (2- and 4-weeks post-treatment).

Rat models have several advantages, such as being easy to handle, available, inexpensive and with a high bone turnover rate. The surgically and chemically induced rat models of osteoarthritis are widely reported^[27]. Since early phases of bone healing are of prime concern in this study, a period of 2-4 weeks post-treatment was deemed satisfactory to evaluate bone regeneration progress in rat model, since the bone remodeling in rats is about 3-4 times faster than human^[28,29]. The contralateral side of the

TMJ was chosen as untreated control in the present study to minimize any anatomical variation between different animals, ensure controlled conditions and prevent the risk of any variants that may affect the outcome of treatment^[30]. We also included normal and osteoarthritic controls.

Osteoarthritis was induced in rats by using MIA in a dose of 2mg for 4 weeks. This is in accordance to Wang XD *et al.*^[16] who stated that mice received 2mg MIA for 4 weeks (a period equivalent to about 3 -4 years in humans) exhibited typical osteoarthritis-like lesions including degenerative changes in the condyle, disc and temporal fossa. Following MIA administration, the TMJ showed massive destruction with ankylosis of the condyle. These results are similar to that reported by Molinet *et al.*^[31], who evaluated microscopic changes in rabbit's TMJ osteoarthritis induced by MIA and they reported a decrease in the articular joint thickness. MIA-act by inducing imbalances in gene expression between anabolic and catabolic genes which leads to cartilage degeneration. This imbalance leads to an increase in the catabolic genes (MMP13 and ADAMTS5) and a decrease in the anabolic genes (aggrecan, collagen I & II) in the condylar head, which produces reduction in the number of chondrocytes^[16].

Histological findings of the PRP-treated side showed normal appearance of the disc and the condyle, in line with that reported by Özkan and Menderes^[32], who observed reduced degenerative changes after PRP intra-articular injection in MIA induced osteoarthritis group. Histomorphometric analysis of the mean bone area percentage revealed no significant differences between the PRP-treated side and the normal group. This suggests that PRP induced bone regeneration at a level comparable to normal bone. Moreover, the PRP-treated side reported statistically significant higher values than the untreated side. These findings are in accordance with Kütük, *et al.*^[33], who reported a significant increase in mean proportion of bone regeneration in the PRP group than in the control group in treating TMJ osteoarthritis in rabbits. PRP was proven to promote bone healing in TMJ osteoarthritis due to the release of large numbers of growth factors^[34], including Insulin-like growth factor (IGF-1), that improves the repair of cartilage and subchondral bone^[35] and Transforming growth factor (TGF)- β , which promotes cartilage repair by increasing the expression of collagen type II^[36].

In the present study, Botox-treated sides revealed healing signs where the condylar surface showed organized cellular layers with few mitotic figures. Alternatively, the untreated side showed huge deformation in the architecture of the condyle with matrix discontinuity with focal areas of chondrocytes loss. The results are in agreement with the study carried out by Yaltirik, *et al.*^[37], who investigated the effects of intra-articular injection of Botox in treating MIA-induced TMJ osteoarthritis in rats. Botox treated groups showed relative improvement as compared with untreated MIA group, but without being statistically significant histologically. This is not in accordance with the histomorphometric analysis of the bone area % in the present study, as the Botox-treated side revealed a statistically significant higher mean bone area percentage than the untreated side. This may be due to; that Botox acts by reducing tartrate-resistant acid phosphatase TRAP^[38]. TRAP enzyme is released by multinucleated giant osteoclast^[39,40], with its reduction by Botox implying less bone remodeling.

The histological results of group III (Botox and PRP) showed normal appearance of the temporal bone, intra-articular disc and the condyle layer which appeared with focal loss of chondrocytes in some areas but without mitotic figures or empty lacunae.

This study is considered the first to discuss the use of combined therapy of Botox and PRP in treating TMJ osteoarthritis. Bulam *et al.*^[41] investigated the usage of mixture of BTX-A and PRP for skin mesotherapy in white rabbits. The results have shown that groups that received Botox and PRP mixture showed less BTX-A activity in comparison to the groups that received BTX-A only. The authors hypothesized the reason behind those results to be that PRP results in an inhibitory effect on the action of BTX-A when they are combined. Therefore, the reparative

potential could be attributed to the action of PRP. This hypothesis can support the findings in the present study, as the best regenerative results were demonstrated in the PRP group followed by Botox+ PRP group, then the Botox group. The histomorphometric analysis supported the histological findings as the normal and PRP-treated sides recorded the highest mean bone area percentage, directly followed by Botox + PRP. Moreover, the difference between treated sides of PRP and Botox+ PRP groups was statistically significant.

In the present study CBCT was used to analyze the joint space in the treated and untreated sides in all three groups. The measurement of radiographic joint space width was chosen in the present study as it is considered one of the most accepted and widely-used method of assessing osteoarthritis progression^[42].

In all groups, the treated sides showed higher mean joint space than the untreated side. These results are in accordance with Wang *et al.*^[43] who investigated radiographically the possibility that IL-17 can induce OA in rabbit knee joints. Results displayed typical manifestations of OA radiographically with obvious joint space narrowing as compared to the control group. On the contrary, these results are not in agreement with those reported by Xu *et al.*^[44] who showed an increased joint space volume in osteoarthritis joints over time using ultrasound images.

One of the most important pro-inflammatory cytokines that contribute to the pathophysiology of osteoarthritis is IL-1 β . IL-1 β is considered an important biochemical marker to monitor the progression of osteoarthritis and efficacy of the intervention, since an increased production in IL-1 β results in cartilage degradation^[45]. ELISA analysis for IL-1 β protein expression showed statistically significantly lower mean IL-1 β levels in all treated sides relative to their untreated sides either after 2-or 4-weeks post-treatment. These results are aligned with the study performed by Ali *et al.*^[46], who studied the role of IL-1 β as a potential biomarker for cartilage degradation in patients with internal derangement or osteoarthritis. The elevated levels of IL-1 β in osteoarthritis could be attributed to: during the early stages of osteoarthritis where bone destruction occurs, IL-1 β is not only secreted by macrophages but also by cells of the articular cartilage; chondrocytes and fibroblasts.

MMP-13 is considered one of the most common enzymes studied for cartilage degradation, due to its capacity in cleaving collagen type II which predominates in the articular cartilage^[47]. The treated side of all groups showed a statistically significant lower mean value of MMP-13 levels as compared to the untreated side either after 2- or 4-weeks post-treatment. Moreover, these results are supported by those of Bo *et al.*^[48] who investigated early cartilage degeneration in developmental dysplasia of the hip (DDH) associated with a high incidence of osteoarthritis in rats. The results showed that MMP-13 was highly expressed in the DDH model group. This could be explained by the fact that MMP-13 plays a key role in

the initiation of the shift from normal chondrocytes to the pathological phase, by driving the levels of low-density lipoprotein receptor-related protein-1 in cartilage^[49].

CONCLUSION

The present study results revealed that PRP intra-articular injection showed the highest potential of bone regeneration in the osteoarthritic cartilage, which regenerated the bone tissue to a level comparable to the normal TMJ histology. Moreover, the regime of using both Botox and PRP combined was the first time to be studied in the study herein. This regime also showed promising results following PRP results and better than using Botox alone. These results indicated that combination of Botox and PRP as an intra-articular injection could be a good treatment option to treat cases of TMJ osteoarthritis and should be considered in further research.

ACKNOWLEDGEMENTS

The authors would like to thank Dr. Khaled Mohamed Keraa for performing the statistical data analysis for the results of this study. The authors would also like to express deep gratitude to Dr. Yahya Amer for performing the radiographic analysis and to Dr. Dina Sabry for conducting the biochemical analysis. The authors certify that there was no specific funding for the research and publication of this article.

CONFLICT OF INTERESTS

There are no conflicts of interest.

REFERENCES

1. Wang XD, Zhang JN, Gan YH, Zhou YH. Current Understanding of Pathogenesis and Treatment of TMJ Osteoarthritis. *J Dent Res* 2015;94:666–73. <https://doi.org/10.1177/0022034515574770>.
2. Peck CC, Goulet JP, Lobbezoo F, Schiffman EL, Alstergren P, Anderson GC, *et al.* Expanding the taxonomy of the diagnostic criteria for temporomandibular disorders. *J Oral Rehabil* 2014;41:2–23. <https://doi.org/10.1111/joor.12132>.
3. Nayyar P, Kumar P, Nayyar PV, Singh A. Botox: Broadening the horizon of dentistry. *J Clin Diagnostic Res* 2014;8: ZE25–9. <https://doi.org/10.7860/JCDR/2014/11624.5341>.
4. Yadav S, Yang Y, Dutra EH, Robinson JL, Wadhwa S, Associate P. Temporomandibular joint disorders in the elderly and aging population. *J Am Geriatr Soc* 2018;66:1213–7. <https://doi.org/10.1111/jgs.15354>. Temporomandibular.
5. Kanchanatawan W, Arirachakaran A, Chaijenkij K, Prasathaporn N, Boonard M, Piyapittayanun P, *et al.* Short-term outcomes of platelet-rich plasma injection for treatment of osteoarthritis of the knee. *Knee Surgery, Sport Traumatol Arthrosc* 2016;24:1665–77. <https://doi.org/10.1007/s00167-015-3784-4>.
6. Cook CS, Smith PA. Clinical Update: Why PRP Should Be Your First Choice for Injection Therapy in Treating Osteoarthritis of the Knee. *Curr Rev Musculoskelet Med* 2018;11:583–92. <https://doi.org/10.1007/s12178-018-9524-x>.
7. Siengdee P, Radeerom T, Kuanon S, Euppayo T, Pradit W, Chomdej S, *et al.* Effects of corticosteroids and their combinations with hyaluronan on the biochemical properties of porcine cartilage explants. *BMC Vet Res* 2015;11. <https://doi.org/10.1186/s12917-015-0611-6>.
8. Perkins C, Whiting B, Lee PY. Steroids and Osteoarthritis. *J Arthritis* 2017;06. <https://doi.org/10.4172/2167-7921.1000e115>.
9. Smyth NA, Murawski CD, Fortier LA, Cole BJ, Kennedy JG. Platelet-Rich Plasma in the Pathologic Processes of Cartilage: Review of Basic Science Evidence. *Arthrosc J Arthrosc Relat Surg* 2013;29:1399–409. <https://doi.org/10.1016/j.arthro.2013.03.004>.
10. Kon E, Filardo G, Di Matteo B, Marcacci M. PRP For the Treatment of Cartilage Pathology. *Open Orthop J* 2013;7:120–8. <https://doi.org/10.2174/1874325001307010120>.
11. Forogh B, Mianehsaz E, Shoaee S, Ahadi T, Raissi GR, Sajadi S. Effect of single injection of platelet-rich plasma in comparison with corticosteroid on knee osteoarthritis: a double-blind randomized clinical trial. *J Sports Med Phys Fitness* 2016;56:901–8.
12. Nayyar P, Kumar P, Nayyar PV, Singh A. BOTOX: Broadening the Horizon of Dentistry. *J Clin Diagn Res* 2014;8:ZE25-9. <https://doi.org/10.7860/JCDR/2014/11624.5341>.
13. Khenioui H, Houvenagel E, Catanzariti JF, Guyot MA, Agnani O, Donze C. Usefulness of intra-articular botulinum toxin injections. A systematic review. *Jt Bone Spine* 2016;83:149–54. <https://doi.org/10.1016/j.jbspin.2015.10.001>.
14. Hegab AF, Ali HE, Elmasry M, Khallaf MG. Platelet-rich plasma injection as an effective treatment for temporomandibular joint osteoarthritis. *J Oral Maxillofac Surg* 2015;73:1706–13. <https://doi.org/10.1016/j.joms.2015.03.045>.
15. Mor N, Tang C, Blitzer A. Temporomandibular myofascial pain treated with botulinum toxin injection. *Toxins (Basel)* 2015;7:2791–800. <https://doi.org/10.3390/toxins7082791>.
16. Wang XD, Kou XX, He DQ, Zeng MM, Meng Z, Bi RY, *et al.* Progression of Cartilage Degradation, Bone Resorption and Pain in Rat Temporomandibular Joint Osteoarthritis Induced by Injection of Iodoacetate. *PLoS One* 2012;7:1–12. <https://doi.org/10.1371/journal.pone.0045036>.

17. Yaltirik M, Palancıoğlu A, Yanar K and, Tuğrul Turgut C. Intraarticular Injections Experimentally Induced Osteoarthritis in Rat Temporomandibular Joint. *J Dent Oral Biol* 2017;2.
18. Allen KD, Adams SB, Mata BA, Shamji MF, Gouze E, Jing L, *et al.* Gait and behavior in an IL1 β -mediated model of rat knee arthritis and effects of an IL1 antagonist. *J Orthop Res* 2011;29:694–703. <https://doi.org/10.1002/jor.21309>.
19. Mabey T, Honsawek S. Cytokines as biochemical markers for knee osteoarthritis. *World J Orthop* January 2015;18:95–105. <https://doi.org/10.5312/wjo.v6.i1.95>.
20. Parasuraman S, Raveendran R, Kesavan R. Blood sample collection in small laboratory animals. *J Pharmacol Pharmacother* 2010;1:87–93. <https://doi.org/10.4103/0976-500X.72350>.
21. Bhatia A, Bs R, Biligi DS, Bk PP. Comparison of different methods of centrifugation for preparation of platelet-rich plasma (PRP). *Indian J Pathol Oncol* 2016;3:535–9. <https://doi.org/10.5958/2394-6792.2016.00099.5>.
22. Maghsoudi O. Standardization and Modification Techniques of Platelet-Rich Plasma (PRP) Preparation in Rabbit. *Int Clin Pathol J* 2015;1:1–5. <https://doi.org/10.15406/icpj.2015.01.00007>.
23. Allen-Worthington KH, Brice AK, Marx JO, Hankenson FC. Intraperitoneal Injection of Ethanol for the Euthanasia of Laboratory Mice (*Mus musculus*) and Rats (*Rattus norvegicus*). *J Am Assoc Lab Anim Sci* 2015;54:769–78.
24. Bancroft, J.D. and Gamble M. *Theory and Practice of Histological Techniques*. 6th ed. Churchill Livingstone, Elsevier, China; 2008.
25. Bancroft JD, Gamble M. *Theory and Practice of Histological Techniques*. Churchill Livingstone; 2002.
26. Wu Y, Goh EL, Wang D, Ma S. Novel treatments for osteoarthritis: An update. *Open Access Rheumatol Res Rev* 2018;10:135–40. <https://doi.org/10.2147/OARRR.S176666>.
27. McCoy AM. Animal Models of Osteoarthritis. *Vet Pathol* 2015;52:803–18. <https://doi.org/10.1177/0300985815588611>.
28. Marsell R, Einhorn TA. The biology of fracture healing. *Injury* 2011;42:551–5. <https://doi.org/10.1016/j.injury.2011.03.031>.
29. Bundkirchen K, Macke C, Reifenrath J, Schäck LM, Noack S, Relja B, *et al.* Severe Hemorrhagic Shock Leads to a Delayed Fracture Healing and Decreased Bone Callus Strength in a Mouse Model. *Clin Orthop Relat Res* 2017;475:2783–94. <https://doi.org/10.1007/s11999-017-5473-8>.
30. Coskun U, Candirli C, Kerimoglu G, Taskesen F. Effect of platelet-rich plasma on temporomandibular joint cartilage wound healing: Experimental study in rabbits. *J Cranio-Maxillofacial Surg* 2019;47:357–64. <https://doi.org/10.1016/j.jcms.2018.12.004>.
31. Molinet M, Alves N, Vasconcelos A, Deana NF. Comparative study of osteoarthritis (OA) induced by monoiodoacetate (MIA) and papain in rabbit temporomandibular joints: macroscopic and microscopic analysis. *Folia Morphol (Warsz)* 2019. <https://doi.org/10.5603/fm.a2019.0104>.
32. Özkan HS, Menderes A. Effects of Intra-Articular PlateletRich Plasma Administration in Temporomandibular Joint Arthritis: An Experimental Study. *Meandros Med Dent J* 2018;19:198–204. <https://doi.org/10.4274/meandros.29484>.
33. Kütük N, Baş B, Soylu E, Gönen ZB, Yilmaz C, Balcıoğlu E, *et al.* Effect of platelet-rich plasma on fibrocartilage, cartilage, and bone repair in temporomandibular joint. *J Oral Maxillofac Surg* 2014;72:277–84. <https://doi.org/10.1016/j.joms.2013.09.011>.
34. Kütük N, Baş B, Soylu E, Gönen ZB, Yilmaz C, Balcıoğlu E, *et al.* Effect of platelet-rich plasma on fibrocartilage, cartilage, and bone repair in temporomandibular joint. *J Oral Maxillofac Surg* 2014;72:277–84. <https://doi.org/10.1016/j.joms.2013.09.011>.
35. Liu XW, Hu J, Man C, Zhang B, Ma YQ, Zhu SS. Insulin-like growth factor-1 suspended in hyaluronan improves cartilage and subchondral cancellous bone repair in osteoarthritis of temporomandibular joint. *Int J Oral Maxillofac Surg* 2011;40:184–90. <https://doi.org/10.1016/j.ijom.2010.10.003>.
36. Timur UT, Caron M, Van Den Akker G, Van Der Windt A, Visser J, Van Rhijn L, *et al.* Increased TGF- β and BMP Levels and Improved Chondrocyte-Specific Marker Expression In *Vitro* under Cartilage-Specific Physiological Osmolarity. *Int J Mol Sci Artic Int J Mol Sci* 2019;20:795. <https://doi.org/10.3390/ijms20040795>.
37. Yaltirik M, Palancıoğlu A, Yanar K, Turgut CT, Bilgic B. The Effects of Intra-Articular Injections of Botulinum Toxin A on Experimentally Temporomandibular Joint Osteoarthritis Models. *Clin Exp Heal Sci* 2018;8:9–13. <https://doi.org/10.5152/clinexphealthsci.2017.424>.
38. Silveira JO, Costa FO, Oliveira PAD, Dutra BC, Cortelli SC, Cortelli JR, *et al.* Effect of non-surgical periodontal treatment by full-mouth disinfection or scaling and root planing per quadrant in halitosis???a randomized controlled clinical trial. *Clin Oral Investig* 2016:1–8. <https://doi.org/10.1007/s00784-016-1959-0>.

39. Glenske K, Wagner AS, Hanke T, Cavalcanti-Adam EA, Heinemann S, Heinemann C, *et al.* Bioactivity of xerogels as modulators of osteoclastogenesis mediated by connexin 43. *Biomaterials* 2014;35:1487–95. <https://doi.org/10.1016/j.biomaterials.2013.11.002>.
40. Bernhardt A, Koperski K, Schumacher M, Gelinsky M. Relevance of osteoclast-specific enzyme activities in cell-based *in vitro* resorption assays. *Eur Cells Mater* 2017;33:28–42. <https://doi.org/10.22203/eCM.v033a03>.
41. Bulam H, Ayhan S, Sezgin B, Zinnuroglu M, Konac E, Varol N, *et al.* The Inhibitory Effect of Platelet-Rich Plasma on Botulinum Toxin Type-A: An Experimental Study in Rabbits. *Aesthetic Plast Surg* 2015;39:134–40. <https://doi.org/10.1007/s00266-014-0418-z>.
42. Hunter A, Kalathingal S. Diagnostic imaging for temporomandibular disorders and orofacial pain. *Dent Clin North Am* 2013;57:405–18. <https://doi.org/10.1016/j.cden.2013.04.008>.
43. Wang L, Wang K, Chu X, Li T, Shen N, Fan C, *et al.* Intra-articular injection of Botulinum toxin A reduces neurogenic inflammation in CFA-induced arthritic rat model. *Toxicon* 2017;126:70–8. <https://doi.org/10.1016/j.toxicon.2016.11.009>.
44. Xu H, Bouta EM, Wood RW, Schwarz EM, Wang Y, Xing L. Utilization of longitudinal ultrasound to quantify joint soft-tissue changes in a mouse model of posttraumatic osteoarthritis. *Bone Res* 2017;5. <https://doi.org/10.1038/boneres.2017.12>.
45. Mabey T, Honsawek S. Cytokines as biochemical markers for knee osteoarthritis. *World J Orthop* 2015;6:95–105. <https://doi.org/10.5312/wjo.v6.i1.95>.
46. Hussain AA, Ghafory Ali B. Evaluation of Interleukin 1 β Levels in Gingival Crevicular Fluid and Serum of Patients with Gingivitis and Chronic Periodontitis. *IOSR J Dent Med Sci* 2014;13:70–5. <https://doi.org/10.9790/0853-131167075>.
47. Rose BJ, Kooyman DL. A Tale of Two Joints: The Role of Matrix Metalloproteases in Cartilage Biology. *Dis Markers* 2016;2016. <https://doi.org/10.1155/2016/4895050>.
48. Bo N, Peng W, Xinghong P, Ma R. Early cartilage degeneration in a rat experimental model of developmental dysplasia of the hip. *Connect Tissue Res* 2012;53:513–20. <https://doi.org/10.3109/03008207.2012.700346>.
49. Yamamoto K, Okano H, Miyagawa W, Visse R, Shitomi Y, Santamaria S, *et al.* MMP-13 is constitutively produced in human chondrocytes and co-endocytosed with ADAMTS-5 and TIMP-3 by the endocytic receptor LRP1. *Matrix Biol* 2016;56:57–73. <https://doi.org/10.1016/j.matbio.2016.03.007>.

المخلص العربي

القدرة الإصلاحية للبوتوكس مجتمع و غير مجتمع مع الصفائح الدموية الغنية بالبلازما في علاج الالتهاب المحدث للمفصل الفكي في الجرذان البيضاء

دينا محمد مكاوي^١، ناهد صدقي قرني^٢، نهاد سمير طه^١، مروة مجدي سعد^٢

^١قسم بيولوجيا الفم، بكلية الطب الفم والاسنان، جامعة مصر الدولية

^٢قسم بيولوجيا الفم، بكلية الطب الفم والاسنان، جامعة القاهرة

أجريت هذه الدراسة لاستقصاء التأثير المضاد للالتهابات والإمكانات العلاجية للبلازما الغنية بالصفائح الدموية، والبوتوكس، ومزيج من كليهما في علاج التهاب المفصل الفكي الصدغي المستحث في الفئران البيضاء. استندت البيانات على الفحوصات النسيجية وفحوص الكيمياء الحيوية.

وقد أُجريت الجزء التجريبي على ٤٢ من الفئران الأصحاء البالغين الذكور الذين تتراوح أعمارهم بين ٣ إلى ٤ أشهر مع متوسط وزن الجسم ١٨٠-٢٠٠ جرام في هذه الدراسة. في المجموعات التجريبية، تم تخدير جميع الفئران بشكل عام عن طريق الحقن داخل الصفاق بواسطة هيدرات الكلورال (٣٧٠-٤٠٠ مجم / جم من وزن الجسم). ثم حُقنت جميع الفئران في الجانب الأيمن والأيسر من المفصل الفكي الصدغي من كل مجموعة بواسطة ٢ مجم من اليود أحادي الصوديوم للحث على التهاب المفاصل العظمي في الجزء العلوي من المفصل الفكي الصدغي.

بعد أحداث التهاب المفاصل وتأكيده من خلال التحليل الكيميائي الحيوي، قُسمت الفئران إلى ٣ مجموعات متساوية (عدد ١٤ فأر لكل مجموعة). المجموعات الثلاث كانت بمثابة المجموعات التجريبية (بعد مرور ٤ اسابيع) وقُسمت وفقاً لنوع العلاج المحقون في الجانب الأيمن من المفصل الفكي الصدغي كما يلي:

- المجموعة الأولى: (مجموعة البوتوكس):
- تم حقن جميع الفئران في هذه المجموعة بتوكسين البوتولينوم أ كحقن داخل المفصل بشكل أسبوعي بمقدار ٥ وحدات دولية / كجم في الجانب الأيمن من المفصل الفكي الصدغي.
- المجموعة الثانية: (مجموعة البلازما الغنية بالصفائح الدموية):
- تم حقن جميع الفئران من هذه المجموعة بواسطة البلازما الغنية بالصفائح الدموية كحقن داخل المفصل بشكل أسبوعي بقدر ٥٠ ميكرو لتر في الجانب الأيمن من المفصل الفكي الصدغي.
- المجموعة الثالثة: (مجموعة البوتوكس + البلازما الغنية بالصفائح الدموية):
- تم حقن جميع الفئران من هذه المجموعة بواسطة البلازما الغنية بالصفائح الدموية بقدر ٥٠ ميكرو لتر في الجانب الأيمن من المفصل الفكي الصدغي، تليها توكسين البوتولينوم أ كحقن داخل المفصل الأسبوعي بقدر ٥ وحدة دولية / كجم في الجانب الأيمن من المفصل الفكي الصدغي.
- تم حقن جميع الفئران أيضاً بـ ٠,٠٥ مل من المياه المالحة في الجانب الأيسر من المفصل الفكي الصدغي كحقن داخل المفصل بشكل أسبوعي.
- بعد مرور ٤ اسابيع تم قُتل عدد ٢ من الفئران من كل مجموعة ليقوموا بدور مجموعة التهاب المفصل العظمي ولتأكيد

حدوث التهاب المفاصل عن طريق الفحوصات النسيجية وفحوصات الكيمياء الحيوية. ثم تم قُتِل عدد ٦ من الفئران الفران بالموت الرحيم عن طريق الحقن داخل الصفاق بـ ٢٠٠ مجم / كجم فينوباربيتال الصوديوم عند ٢ و ٤ أسابيع بعد تأكيد حدوث التهاب المفاصل. ثم سُرحت العينات، وقُسمت وتُبِتت في الفورمالين ١٠ ٪، وتم نزع الكالسيوم بوضعها في ١٤ ٪ إيديتات لمدة ٦-٨ أسابيع وأخيرا وُضعت من أقسام شمع البارافين. بعدها تمت دراسة الأجزاء التي تم الحصول عليها. كشف الفحص الحالي النتائج التالية

أ. نسبة مساحة العظام (حجم أنسجة العظام / إجمالي حجم الأنسجة)

- في جميع المجموعات، إما بعد ٢ أو ٤ أسابيع، أظهر الجانب التجريبي نسبة متوسط مساحة العظام أعلى بكثير من الناحية الإحصائية من جانب مجموعات المقارنة.
- بالمقارنة بين المجموعات، سجلت مجموعة البلازما الغنية بالصفائح الدموية في الجانب التجريبي أعلى قيمة متوسط ذات دلالة إحصائية بعد ٢ أو ٤ أسابيع.

ب. مخروط شعاع التصوير المقطعي (CBCT)

في المقارنه بين المجموعات المختلفة ، أظهر الجانب التجريبي قيمة متوسط اعلى و ذو دلالة إحصائية في قياس مسافة المفصل عن جانب مجموعات المقارنة في مجموعة البوتكس و ذو دلالة غير إحصائية في مجموعتي البلازما الغنية بالصفائح الدموية و مجموعة البوتوكس + البلازما الغنية بالصفائح الدموية.

ت. مقايسة الممتز المناعي المرتبط بالإنزيم مع جين إنترلوكين - ١ بتا

١. في جميع المجموعات، إما بعد ٢ أو ٤ أسابيع، أظهر الجانب التجريبي انخفاضا ملحوظا ذات دلالة إحصائية في مستوى بروتين إنترلوكين - ١ بتا عن مستوياته في جانب المجموعة المقارنة.

ث. تفاعل البلمرة المتسلسل الوقتي

١. في كل المجموعات، إما بعد ٢ أو ٤ أسابيع، أظهر الجانب التجريبي انخفاضا ملحوظا ذو دلالة إحصائية في متوسط مستويات إنزيم MMP١٣ عن جانب مجموعات المقارنة.